Published in final edited form as:
Brain Res. 2011 April 12; 1384: 15–22. doi:10.1016/j.brainres.2011.02.014.

Brain Glucose Transporter (Glut3) Haploinsufficiency Does Not Impair Mouse Brain Glucose Uptake

Charles A. Stuart[1], **Ian R. Ross**[1], **Mary E. A. Howell**[1], **Melanie P. McCurry**[1], **Thomas G. Wood**[2], **Jeffrey D. Ceci**[2], **Stephen J. Kennel**[3], and **Jonathan Wall**[3]

[1]East Tennessee State University Quillen College of Medicine, Johnson City, Tennessee

[2]The University of Texas Medical Branch at Galveston, Galveston, Texas

[3]The Preclinical and Diagnostic Molecular Imaging Laboratory of The University of Tennessee Graduate School of Medicine, Knoxville, Tennessee

Abstract

Mouse brain expresses three principle glucose transporters. Glut1 is an endothelial marker and is the principal glucose transporter of the blood-brain barrier. Glut3 and Glut6 are expressed in glial cells and neural cells. A mouse line with a null allele for Glut3 has been developed. The *Glut3*−/− genotype is intrauterine lethal by seven days post-coitis, but the heterozygous (*Glut3*+/−) littermate survives, exhibiting rapid post-natal weight gain, but no seizures or other behavioral aberrations. At twelve weeks of age, brain uptake of tail vein-injected ^{3}H-2-deoxy glucose in *Glut3*+/− mice was not different from *Glut3*+/+ littermates, despite 50% less Glut3 protein expression in the brain. The brain uptake of injected ^{18}F-2-fluoro-2-deoxy glucose was similarly not different from *Glut3*+/− littermates in the total amount, time course, or brain imaging in the *Glut3*+/− mice. Glut1 and Glut6 protein expressions evaluated by immunoblots were not affected by the diminished Glut3 expression in the *Glut3*+/− mice. We conclude that a 50% decrease in Glut3 is not limiting for the uptake of glucose into the mouse brain, since *Glut3* haploinsufficiency does not impair brain glucose uptake or utilization.

Keywords

Glut3; brain; glucose uptake; Glut1; Glut6

1. Introduction

Facilitative hexose transporters are part of a family of solute carriers termed SLC2 with 14 different isoforms, most of which are designated GLUT's and transport glucose (Joost, et al., 2002). The first of these proteins, GLUT1, was identified and cloned in 1985. The third member, GLUT3, was also named the "brain glucose transporter" because it was expressed at high levels in nerves and neural tissue. GLUT3 is also found at lower expression levels in many other tissues, including muscle and fat (Bell, et al., 1993). Like many of the proteins

Corresponding Author: Charles A. Stuart, MD, East Tennessee State University, Quillen College of Medicine, PO Box 70622, Johnson City, Tennessee 37614-0622, 423-439-6282, Fax 423-439-6387, stuartc@etsu.edu .

of this family, GLUT3 is expressed primarily on the cell surface and is not acutely regulated by insulin in the "insulin-sensitive" tissues, muscle and fat (Scheepers, et al., 2004). Since it is likely that GLUT3 provides at least a portion of the basal glucose uptake in muscle and fat (Simpson, et al., 2008;Stuart, et al., 2001), we developed a *Glut3* knockout mouse line to investigate the impact on insulin responsiveness of diminished basal glucose uptake in muscle and fat. In agreement with other reports (Ganguly, et al., 2007;Schmidt, et al., 2009), the *Glut3*−/− conceptus in our line does not survive beyond E7 days post-coitis (dpc), but the heterozygous littermates survive and are fertile (Stuart, et al., 2007). As part of the characterization of the phenotype of the *Glut3*+/− mice, we documented that Glut3 protein expression in brain was 50% of that of the *Glut3*+/+ littermates. To our surprise, there was no change in behavior or seizure activity as seen in *Glut1*+/− mice, even with prolonged fasting in the heterozygous mice. This report details our investigation of the brain glucose uptake in Glut3+/− mice.

2. Results

2.1. Expression of Glut1, Glut3, and Glut6 in *Glut3*+/− mouse brain

Figure 1 displays sample immunoblots of mouse brain homogenate probed with antibodies directed against mouse Glut3, human GLUT1, and human GLUT6. The GLUT1 antibody is fully active against mouse Glut1 since the 12 amino acid peptide used to generate the antibody is identical to the carboxy terminus of both human and mouse. The GLUT6 antibody was generated with a 16 amino acid peptide that has 56% identity with the mouse carboxy terminal sequence. This antibody was specifically reactive with the mouse Glut6. The *Glut3*+/− mouse brain contained 52% of the level of signal seen in the *Glut3*+/+ littermates. Neither Glut1 nor Glut6 immunoblots indicated any increase in expression in the *Glut3*+/− as compared to homogenate from *Glut3*+/+ mouse brains. Glut1 expression in *Glut3*+/− mice averaged 16% less and Glut6 was 15% more than *Glut3*+/+ littermates, but neither of these differences were statistically significant. Thus, no evidence was found for compensatory post-translational increase in Glut3 expression or compensation through increases in either of the other two principal glucose transporters expressed in brain.

2.2. Prolonged fasting of *Glut3*+/− mice results in decreased blood glucose concentrations but no observable seizure activity

Since heterozygous defects in the *GLUT1* gene are associated with a 50% decrease in GLUT1 and neonatal seizures in humans (De Vivo, et al., 1991) and mice (Wang, et al., 2006), we speculated that a similar decrease in Glut3 expression in brain might parallel the effects of a 50% decrease in the glucose transporter that constitutes the blood-brain barrier (Glut1). Male and female mice with Glut3+/− or Glut3+/+ genotypes were subjected to restricted food access in order to decrease the blood glucose concentration and cause a decrease in the cerebro-spinal fluid concentration of glucose. Figure 2 displays the changes that occurred in blood glucose in animals subjected to food deprivation up to 48 hours. Ambient temperature in the animal care facility room was maintained at 29°C for six weeks in order to minimize the decrease in physical activity that occurs with limited food. By 24 hours, blood glucose declined to 60-80 mg/dL, about half of that of the ad lib fed mice at the beginning of this study. The activity of the mice decreased with food deprivation, but there was no evidence of seizure activity or behavior arrest and the behavior of the mice was otherwise indistinguishable between *Glut3*+/− and *Glut3*+/+ genotypes.

2.3. Uptake of ^{3}H-2-deoxyglucose in *Glut3*+/− mouse brain after tail injection

Five males and five females with the Glut3+/− genotype were injected with 2 μCi of ^{3}H-2-deoxy glucose via tail vein. After 45 minutes, the brains were harvested and processed as described in *Methods*. Studies performed on three separate occasions were pooled using the

mean of the counts from brains from the *Glut3*+/+ mice to normalize the data. The data displayed in Figure 3 are counts per whole brain, but expressing the data as counts per gram brain weight did not alter the result of the comparison. The difference between the two groups (13% less in *Glut3*+/−) was not statistically significant.

2.4. MicroPET/CT imaging of mice

Representative co-registered PET/CT images revealed no differences in the gross distribution of ^{18}F-FDG in Glut3+/+ and Glut3+/− mice as shown in Figure 4. Clearly visible was uptake in the brain, heart (myocardium), kidneys (catabolism and clearance), Harderian glands, and bladder (clearance). There was also diffuse blood pool activity visible in the liver. The field of view of the PET images was greater than that for the CT data, which accounts for the apparent PET activity outside the limits of the CT image – the area from the bladder to the Harderian glands is shown.

2.5. Kinetic analysis of ^{18}F-FDG data

Figure 4B displays the time course of ^{18}F-FDG uptake in the brain and liver regions of interest from two representative mice. The dynamic data were analyzed using both a single compartment (Table 1) and 2-compartment model (Table 2) with reversible binding. In short, the K1 rate constant describes the movement of the ^{18}F-FDG tracer from the blood to compartment 1 (cells within the brain). This rate is dependent upon the expression and type of glucose transporter proteins in the whole brain. Statistical evaluation of the K1 rates using a Mann-Whitney test revealed no significant difference ($P > 0.10$) between the mean values estimated from either the 1 compartment model (0.235 ± 0.038 ml/cm^3/min, 90% confidence interval 0.147-0.323 for *Glut3*+/+ mice and 0.178 ± 0.018 ml/cm3/min, 90% confidence interval 0.136-0.226 for *Glut3*+/− mice) or the 2 compartment model (0.776 ± 0.147 ml/cm^3/min, 90% confidence interval 0.430-1.122 for *Glut3*+/+ mice and 0.624 ± 0.032 ml/cm3/min, 90% confidence interval 0.549-0.699 for *Glut3*+/− mice).

Similarly, the mean and median values calculated for the K1 rate constant and the cerebral glucose metabolic rates (CMR_{gluc}) using the 2-compartment model (appropriate for FDG) were essentially identical in both the Glut3+/+ and *Glut3*+/− mice (36.3 ± 4.25, 90% confidence interval 26.3-46.3 for *Glut3*+/+ mice and 35.4 ± 4.77, 90% confidence interval 24.2-46.6 for *Glut3*+/− mice). Note that the data for mouse 475(Glut3+/+) was omitted from the analyses because the injection was made before the onset of data acquisition.

3. Discussion

Despite a decrease in brain Glut3 expression that was proportional to the loss of one allele of the *Glut3* gene, there was no evidence of diminished brain uptake of glucose as indicated by brain uptake of ^{3}H-2-deoxy glucose or as quantified by detailed kinetics and imaging of ^{18}F-FDG uptake assessed by dynamic PET imaging. There was no evidence of increased expression of Glut1 or Glut6 transporter proteins to compensate for the loss of 50% of the Glut3 protein found in the normal brain. These data suggest that half of the normal expression of the brain transporter, Glut3 with its high affinity for glucose (Simpson, et al., 2008) is sufficient to provide normal glucose entry into the neural cells of the brain even when peripheral blood concentrations of glucose are substantially reduced by food restriction.

The distribution of ^{18}F-FDG in Glut3 heterozygous knockout (*Glut3*+/−) mice and littermate *Glut3*+/+ animals was essentially equivalent as evidenced in the coregistered PET/CT images. Notably, activity was observed in the myocardium, brain and Harderian glands with evidence of normal tracer clearance in the kidneys and bladder.

The dynamic accumulation of glucose in the brain of heterozygous Glut3 knockout mice and Glut3+/+ counterparts was analyzed using compartmental modeling of the ^{18}F-FDG data. The region of interest (ROI) drawn over the brain to generate the time activity curve was placed toward the hindbrain to ensure that activity from the Harderian glands did not spill over into the monitored region. To perform these analyses a whole blood input function is required and was generated by placing a second ROI in the liver of each mouse. The data were analyzed using either a 1- or 2-compartment model. The 2-compartment model best approximates the accumulation of FDG. However, in both models, K1 represents the rate constant associated with uptake of the tracer from the blood. In both models, this is expressed as a reversible equilibrium. In the 2-compartment model, the second compartment denotes the metabolic product of FDG following phosphorylation by hexokinase.

In this respect, K1 in both models is linked to the uptake of tracer from the blood pool and therefore is related to the type and concentration of glucose transporter proteins present in the tissue. For this reason we analyzed the K1 values calculated in each model for *Glut3*+/− and *Glut3*+/+ mice. There were no significant differences between the two mouse populations identified using the t-test and Mann-Whitney analyses. Similarly, the mean and median values for the K1 rate constants and cerebral metabolic glucose rates (CMR's) were essentially indistinguishable. The CMR values that we have calculated are consistent with previous measurements. Normoglycemic mice under isoflurane anesthesia have CMR values of ~24 and ~29 in the frontal and occipital cortices, respectively (Wu, et al., 2007). In addition, rates of 0.8 – 0.13 mL/min/g have been reported for K1 in the whole brain of mice under isoflurane anesthesia (Toyama, et al., 2004). Toyama and coworkers noted that general anesthesia may decrease mouse brain glucose uptake but this effect is minimized with isoflurane. The CMR values calculated in this study are within acceptable limits; however the K1 rates all appear a little high relative to the published range. This, and other discrepancies or errors, may be due to the fact that i) in the absence of data on the glucose levels of the mice when they were scanned, an arbitrary value of 5.0 mM was used, ii) the whole-blood input function we used for the analyses was estimated based upon the region where the aorta is located as it passes dorsal to the liver in the abdomen in each mouse; iii) the region of the brain selected for the circular ROI was determined somewhat arbitrarily, albeit consistently, and comprised a cross section of the entire brain (away from the Harderian glands). Using the analyses we have performed, these data indicate that cerebral glucose metabolism in the *Glut3*+/− mice was not significantly different from littermate *Glut3*+/+ mice.

The distribution of glucose transporters in the brain may be heterogeneous. Early studies of the Glut3 mRNA distribution in Japanese monkey brain showed a higher amount in the frontal lobe (Yano, et al., 1991). Immunologic studies of rat brain showed densities of Glut3 throughout the brain that varied over a two-fold range (Zeller, et al., 1995). In contrast, human brain samples showed similar intensity of GLUT3 protein by immunoblot in most areas of the brain (Haber, et al., 1993). Haber and coworkers found that samples of gray matter from various regions of the human brain contained much more GLUT3 protein as indicated in immunoblots. White matter contained less GLUT3. Cerebellum was less intense than cerebral cortex because it contained a mixture of gray and white matter (Haber, et al., 1993). The distribution in brain and regulation of Glut1 and Glut3 seem quite different (Duelli and Kuschinsky, 2001). The distribution of Glut1 and Glut3 generally follow the distribution of brain capillaries and the relative amount of ^{3}H-2-deoxy glucose uptake (Duelli and Kuschinsky, 2001), but Leino and coworkers have demonstrated by immuno-electron microscopy that Glut1 is expressed in capillary endothelial cells and astrocytes but not neurons, whereas Glut3 is exclusively expressed in neurons, primarily in pre- and postsynaptic nerve ending (Leino, et al., 1997). In rats, one week of insulin-induced hypoglycemia slightly increased Glut3, but not Glut1, and three weeks of hyperglycemia

from streptozotocin-induced diabetes slightly decreased Glut1, but did not affect Glut3 expression (Duelli and Kuschinsky, 2001). Based on these previous studies, it is possible that our exclusion of the frontal region of the mouse brain because of the Harderian glands may have missed a significant change in glucose uptake in the PET scans, but the ^{3}H-2-deoxy glucose uptake studies described in Results Section 2.3 used whole brain and the slightly lower glucose uptake was not significantly different from the controls.

Studies performed by Schmidt and coworkers on the heterozygous Glut3 knockout mice they developed did not identify any evidence of neurological dysfunction (Schmidt, et al., 2008). In behavioral testing, they did not find any difference from wild type in coordination, reflexes, motor abilities, learning, or memory. However, they did not report challenging the Glut3+/− mice with fasting. Subtle regional brain dysfunction with a modest decrease in brain glucose uptake may have been missed in these detailed behavioral studies or in our studies where frequent simple observation of activity was the brain function outcome indicator.

Dong Wang and coworkers developed a mouse line that exhibited a defective *Glut1* allele (Wang, et al., 2006) in order to mimic the human Glut1 deficiency syndrome (De Vivo, et al., 1991;Wang, et al., 2005). Like the Glut3 knockout mouse, the homozygous Glut1 defect was embryonic lethal. These investigators found that *Glut1* −/− embryos were smaller with developmental abnormalities at E13 dpc. The mechanism for embryo loss appeared to be related to the inability to transport glucose to the embryo after the time of mature placental formation at E10 dpc (Wang, et al., 2006). Wang and coworkers found electroencephalographic (EEG) evidence of seizure activity in the *Glut1*+/− mice but no physical evidence of seizure activity until these mice were fasted for 24 hours. They documented brief (1-4 seconds) behavior arrest during the EEG rhythmic spike discharges by continuous video/electrographic recordings. We did not monitor electrographically, but there were no behavior arrest periods in the *Glut3*+/− mice or their wild-type littermates.

GLUT1, GLUT3, and GLUT6 are the predominant facilitative glucose transporters expressed in the human brain, making up 97% of the frontal cortex homogenate mRNA for glucose transporting proteins (Stuart, unpublished data), excluding GLUT13 (HMIT) which transports only inositols. GLUT1 has an affinity for glucose that is similar to that or GLUT4 (Kd for d-glucose about 5 mM) (Bell, et al., 1993;Gould and Holman, 1993). In contrast, GLUT3 has a higher affinity with a Kd about 1 mM, and GLUT6 has a lower affinity for d-glucose with a Kd at least twice the level of GLUT4 (Lisinski, et al., 2001), similar to the affinity for d-glucose found for GLUT2 (Bell, et al., 1993). GLUT1 and GLUT3 are constitutively expressed at the cell surface, whereas GLUT4 and GLUT6 are predominantly intracellular in their location (Bell, et al., 1993;Joost and Thorens, 2001;Lisinski, et al., 2001;Stuart, et al., 2009). Insulin causes GLUT4 to translocate to the cell surface in fat and muscle, but Lisinski and coworkers found that insulin does not result in movement of GLUT6 to the cell surface (Lisinski, et al., 2001). They demonstrated that GLUT6 continuously recycles back and forth between the cell surface and an intracellular compartment, by showing accumulation at the cell surface if endocytosis is blocked (Lisinski, et al., 2001). At this time, it is unclear what cell types in the brain express GLUT6, but preliminary data in our lab suggests it is expressed predominantly in nerve cells. How expression of GLUT6 is regulated and what role it plays in nerve cell uptake of glucose is not known.

The results of the studies described here show that even though mice heterozygous for a defective *Glut3* gene have only half as much brain Glut3, glucose uptake into brain tissue is normal. Since there was no evidence of compensation by post-translational effects on Glut3 content or by increased expression of the other principal brain glucose transporters, Glut1

and Glut6, the decreased brain Glut3 content was still sufficient to provide normal glucose uptake into neural tissue. Unlike brain expression of *Glut1*, haploinsufficiency of *Glut3* does not impair brain glucose uptake and is not associated with brain dysfunction. We conclude that Glut3 is normally expressed in mouse brain in excess and the higher affinity of glut3 for glucose protects the brain from low glucose uptake during prolonged starvation or even if there were diminished expression of the Glut3 protein in neural tissues.

4. Materials and Methods

4.1. Materials

Affinity-purified rabbit anti-hGLUT1, anti-mGlut3, and anti-hGLUT6 antibodies were purchased from Alpha Diagnostics (San Antonio, TX). A supply of the peptide used to immunize the animal source was obtained from the vendor of specific antibodies. SuperSignal west pico chemoluminescence substrate was purchased from Pierce (Rockford, IL).

4.2. Development of the *Glut3*−/− mouse line

Briefly, a deletion within exon 2 was introduced and a positive selectable marker for neomycin (neo) resistance under the transcriptional control of the phosphoglycerate kinase (PGK) promoter was inserted into the Glut3 coding region of exon 2. This construct was successfully introduced in a 129 Svj line which was crossed with C57BL/6 to increase litter size. No homozygous *Glut3*−/− pups were found in over 50 matings, indicating intrauterine lethality. Genotyping at weaning revealed that *Glut3*+/+ and *Glut3*+/− pups were born to Glut3+/− Glut3+/− matings in the predicted ratio of 2:1, indicating there was no survival disadvantage for the heterozygous embryos.

4.3. Genotyping

DNA was isolated from tail snips from weaned pups and subjected to PCR with specific primers. Four primers were designed (A:5′-gctctccaggtgaccccatctc, B:5′-ctcactgtctcaggtgcattgatg, C: 5′-tgcagcagactagtgagacgtgc, D:5′-tacattttgaatggaaggattggagc) that generated a 107 bp piece (primers A and B) from the wild type and 294 bp (primers A and C) and 385 bp (primers B and D) fragments from the allele containing the “neo” insertion.

4.4. Prolonged food deprivation

To determine if low blood glucose could result in evidence of inadequate delivery of glucose to the brain tissue of mice with diminished Glut3 expression, extended food deprivation up to 48 hours was performed. Ambient temperature was maintained at 29°C to minimize torpor that can occur with food restriction. Mice were observed for 30 minutes for motor seizures or behavior arrest at the time of blood draws and every six hours in between the blood draws. After ad lib feeding overnight, food was removed and glucose was determined in blood from a cheek puncture at times 0, 6, 12, 24, and 48 h. Only one blood draw was performed at the end of each specified period of food deprivation. Each individual mouse had five blood glucose determinations separated by one week before the next sequentially increased fasting time period. All animal manipulations described herein were performed under the auspices of an Institutional Animal Care and Use Committee-approved protocol at East Tennessee State University, The University of Tennessee Graduate School of Medicine in Knoxville, or at the University of Texas Medical Branch at Galveston.

4.5. Brain uptake of ^{3}H 2-deoxy glucose from maternal circulation

Mice at 10-12 weeks of age were fed ad lib overnight, had food removed two hours prior to study, and then were administered 2 μCi ^{3}H 2-deoxyglucose intravenously via the lateral tail vein with the mouse briefly restrained in apparatus designed for tail vein injection. At 45 minutes after the injection, mice were sacrificed by CO_2 inhalation and the whole brain removed, weighed, placed in scintillation vials containing Scintigest (Fisher Scientific), and slowly agitated at 50° C overnight or until fully dissolved. Liquid scintillation counts were adjusted for quench and expressed as cpm/brain or dpm/g brain weight. Initial time course studies showed brain ^{3}H content increased until 45-60 minutes after injection and then declined (data not shown).

4.6. Immunoblot technique

Immunoblotting was performed essentially as previously described (Stuart, et al., 1999). Twelve-week old mice were allowed ad lib feeding overnight and after sacrifice by CO_2 inhalation, whole brains were removed and quickly frozen in liquid nitrogen for later study. For the GLUTs to be evaluated, 20 μg of whole brain protein from homogenate was separated on a 10% polyacrylamide gel using the Laemmli system (Laemmli, 1970), transferred to a nitrocellulose membrane, subjected to blocking with 2.5% non-fat dry milk in phosphate-buffered saline (PBS), incubated with a validated dilution (1:100 to 1:500) of anti-GLUT antibody dissolved in PBS, 1.25% milk, then anti-rabbit IgG, and developed with enhanced chemiluminescence reagent followed by exposure of the membrane to X-ray film. Quantitative comparisons were performed using digital image analysis with Quantity One software from BioRad.

4.7. MicroPET P4 image acquisition

These studies were performed after overnight ad lib feeding of mouse chow, but food was removed two hours prior to the anesthesia and injections. Mice were anesthetized using 1-2% isoflurane in oxygen with a flow rate of 0.5 L/min. A catheter was placed in the lateral tail vein to allow delivery of ^{18}F-2-fluoro-2-deoxy glucose (^{18}F-FDG). The mouse was placed in a custom built chamber (M2M Imaging Corp., Newark, NJ) and then mounted onto the microPET imaging bed – the animal was maintained on 2% isoflurane throughout the duration of the imaging protocol. The data were acquired using a microPET P4 small animal imaging system (Concorde Microsystems Inc., Knoxville, TN) which offers 7.8 cm axial and 19 cm transaxial fields of view. The system contains 168 detector modules each with an 8×8 LSO crystal-array capable of achieving 1.8 mm spatial resolution.

Dynamic PET data were obtained by ensuring that the start of the image acquisition was coincident with the injection of the ^{18}F-FDG in each mouse. Each mouse was infused with a bolus of between 0.5 – 0.8 mCi of ^{18}F-FDG in a volume of less than 250 μL. Image data were acquired for 30 min using an energy window of 350-650 keV. No scatter or attenuation corrections were performed.

4.8. ^{18}F-FDG Histogramming and reconstruction

The resulting data were reconstructed using 2D-ordered subset expectation maximization (OSEM) algorithm with 16 subsets and 4 iterations. The images were presented on a 128 × 128 × 63 matrix with x, y, z voxel dimensions of 1.9 mm × 1.9 mm × 1.2 mm. This method provided high-quality image output without prohibitively long reconstruction times.

4.9. ^{18}F-FDG Kinetic analysis

The microPET data were evaluated using both 1- and 2-compartment models with reversible binding (Logan, 2000;Patlak and Blasberg, 1985;Patlak, Blasberg, and Fenstermacher,

1983), implemented in the PMOD kinetic analysis software (v 2.9, PMOD Technologies, Zurich, Switzerland). Regions of interest (ROI) were manually drawn on the axial images of the brain and the hepatic aorta to yield the cerebral time activity curve and whole blood input function, respectively. The model was fitted using up to 400 iterations of the Marquardt and Powell algorithms. For these calculations, a glucose concentration of 5.0 mM and a lumped constant of 0.437 were used. The vascular fraction and blood parameters were fitted using all the data points. The calculated rate constants (K1, k2, and k3), cerebral metabolic glucose rate (CMR_{gluc}), and summary statistics are summarized in Tables 1 and 2 below.

4.10. MicroCAT II image acquisition

CT images were obtained using a microCAT II + SPECT small animal imaging system (Siemens Preclinical Solutions, Knoxville, TN). The microCAT II scanner has a circular orbit cone beam geometry, equipped with a 20-80 kVp microfocus x-ray source, and captures a 90 mm × 60 mm field of view using a 2048 × 3072 CCD array detector, optically coupled to a minR phosphor screen via a fiber-optic bundle. The CT data, composed of 360 projections at 1° azimuths, were acquired in 9 min 30 sec using an exposure time of 475 msec per projection. Images were reconstructed in real-time on isotropic 77-μm voxels using an implementation of the Feldkamp backprojection algorithm.

The PET and CT data were manually coregistered using the Amira software package (Amira, Version 3.1: Mercury Computer Systems).

4.11. Statistics

All data are displayed as mean ± standard errors. Comparisons between two groups were performed using Student's t test for independent groups. ANOVA was used for comparisons of three or more independent groups.

Acknowledgments

These studies were funded in part by a grant from the National Institutes of Health DK080488 (Stuart). None of the authors have any financial disclosures.

References

Bell GI, Burant CF, Takeda J, Gould GW. Structure and function of mammalian facilitative sugar transporters. J. Biol. Chem. 1993; 268:19161–19164. [PubMed: 8366068]

De Vivo DC, Trifiletti RR, Jacobson RI, Ronen GM, Behmand RA, Harik SI. Defective glucose transport across the blood-brain barrier as a cause of persistent hypoglycorrhachia, seizures, and developmental delay. N. Engl. J. Med. 1991; 325:703–709. [PubMed: 1714544]

Duelli R, Kuschinsky W. Brain glucose transporters: relationship to local energy demand. News Physiol Sci. 2001; 16:71–76. [PubMed: 11390952]

Ganguly A, McKnight RA, Raychaudhuri S, Shin BC, Ma Z, Moley K, Devaskar SU. Glucose transporter isoform-3 mutations cause early pregnancy loss and fetal growth restriction. Am. J. Physiol Endocrinol. Metab. 2007; 292:E1241–E1255. [PubMed: 17213475]

Gould GW, Holman GD. The glucose transporter family: structure, function and tissue-specific expression. Biochem. J. 1993; 295:329–341. [PubMed: 8240230]

Haber RS, Weinstein SP, O'Boyle E, Morgello S. Tissue distribution of the human GLUT3 glucose transporter. Endocrinology. 1993; 132:2538–2543. [PubMed: 8504756]

Joost HG, Bell GI, Best JD, Birnbaum MJ, Charron MJ, Chen YT, Doege H, James DE, Lodish HF, Moley KH, Moley JF, Mueckler M, Rogers S, Schurmann A, Seino S, Thorens B. Nomenclature of the GLUT/SLC2A family of sugar/polyol transport facilitators. Am. J. Physiol Endocrinol. Metab. 2002; 282:E974–E976. [PubMed: 11882521]

Joost HG, Thorens B. The extended GLUT-family of sugar/polyol transport facilitators: nomenclature, sequence characteristics, and potential function of its novel members (review). Mol. Membr. Biol. 2001; 18:247–256. [PubMed: 11780753]

Laemmli UK. Cleavage of structural proteins during the assembly of the head of bacteriophage T4. Nature. 1970; 227:680–685. [PubMed: 5432063]

Leino RL, Gerhart DZ, Van Bueren AM, McCall AL, Drewes LR. Ultrastructural localization of GLUT1 and GLUT3 glucose transporters in rat brain. J. Neurosci. Res. 1997; 49:617–626. [PubMed: 9302083]

Lisinski I, Schurmann A, Joost HG, Cushman SW, Al Hasani H. Targeting of GLUT6 (formerly GLUT9) and GLUT8 in rat adipose cells. Biochem. J. 2001; 358:517–522. [PubMed: 11513753]

Logan J. Graphical analysis of PET data applied to reversible and irreversible tracers. Nucl. Med. Biol. 2000; 27:661–670. [PubMed: 11091109]

Patlak CS, Blasberg RG. Graphical evaluation of blood-to-brain transfer constants from multiple-time uptake data. Generalizations. J. Cereb. Blood Flow Metab. 1985; 5:584–590. [PubMed: 4055928]

Patlak CS, Blasberg RG, Fenstermacher JD. Graphical evaluation of blood-to-brain transfer constants from multiple-time uptake data. J. Cereb. Blood Flow Metab. 1983; 3:1–7. [PubMed: 6822610]

Scheepers A, Joost HG, Schurmann A. The glucose transporter families SGLT and GLUT: molecular basis of normal and aberrant function. JPEN J. Parenter. Enteral Nutr. 2004; 28:364–371. [PubMed: 15449578]

Schmidt S, Hommel A, Gawlik V, Augustin R, Junicke N, Florian S, Richter M, Walther DJ, Montag D, Joost HG, Schurmann A. Essential role of glucose transporter GLUT3 for post-implantation embryonic development. J. Endocrinol. 2009; 200:23–33. [PubMed: 18948350]

Schmidt S, Richter M, Montag D, Sartorius T, Gawlik V, Hennige AM, Scherneck S, Himmelbauer H, Lutz SZ, Augustin R, Kluge R, Ruth P, Joost HG, Schurmann A. Neuronal functions, feeding behavior, and energy balance in Slc2a3+/− mice. Am. J. Physiol Endocrinol. Metab. 2008; 295:E1084–E1094. [PubMed: 18780771]

Simpson IA, Dwyer D, Malide D, Moley KH, Travis A, Vannucci SJ. The facilitative glucose transporter GLUT3: 20 years of distinction. Am. J. Physiol Endocrinol. Metab. 2008; 295:E242–E253. [PubMed: 18577699]

Stuart CA, Howell ME, Zhang Y, Yin D. Insulin-stimulated translocation of glucose transporter (GLUT) 12 parallels that of GLUT4 in normal muscle. J. Clin. Endocrinol. Metab. 2009; 94:3535–3542. [PubMed: 19549745]

Stuart CA, Howell MEA, Yin D, Copland JA, Wood TG, Ceci JD. The brain glucose transporter (Glut3) null genotype is associated with post-implantation failure of embryo formation. Diabetes. 2007; 56(Supplement 1):A329. Abstract.

Stuart CA, Wen G, Jiang J. GLUT3 protein and mRNA in autopsy muscle specimens. Metabolism. 1999; 48:876–880. [PubMed: 10421229]

Stuart CA, Wen G, Williamson ME, Jiang J, Gilkison CR, Blackwell SJ, Nagamani M, Ferrando AA. Altered GLUT1 and GLUT3 gene expression and subcellular redistribution of GLUT4 protein in muscle from patients with acanthosis nigricans and severe insulin resistance. Metabolism. 2001; 50:771–777. [PubMed: 11436180]

Toyama H, Ichise M, Liow JS, Modell KJ, Vines DC, Esaki T, Cook M, Seidel J, Sokoloff L, Green MV, Innis RB. Absolute quantification of regional cerebral glucose utilization in mice by 18F-FDG small animal PET scanning and 2-14C-DG autoradiography. J. Nucl. Med. 2004; 45:1398–1405. [PubMed: 15299067]

Wang D, Pascual JM, Yang H, Engelstad K, Jhung S, Sun RP, De Vivo DC. Glut-1 deficiency syndrome: clinical, genetic, and therapeutic aspects. Ann. Neurol. 2005; 57:111–118. [PubMed: 15622525]

Wang D, Pascual JM, Yang H, Engelstad K, Mao X, Cheng J, Yoo J, Noebels JL, De Vivo DC. A mouse model for Glut-1 haploinsufficiency. Hum. Mol. Genet. 2006; 15:1169–1179. [PubMed: 16497725]

Wu HM, Sui G, Lee CC, Prins ML, Ladno W, Lin HD, Yu AS, Phelps ME, Huang SC. In vivo quantitation of glucose metabolism in mice using small-animal PET and a microfluidic device. J. Nucl. Med. 2007; 48:837–845. [PubMed: 17475972]

Yano H, Seino Y, Inagaki N, Hinokio Y, Yamamoto T, Yasuda K, Masuda K, Someya Y, Imura H. Tissue distribution and species difference of the brain type glucose transporter (GLUT3). BBRC. 1991; 174:470–477. [PubMed: 1704223]

Zeller K, Duelli R, Vogel J, Schröck H, Kuschinsky W. Autoradiographic analysis of the regional distribution of Glut3 glucose transporters in the rat brain. Brain Res. 1995; 698:175–179. [PubMed: 8581478]

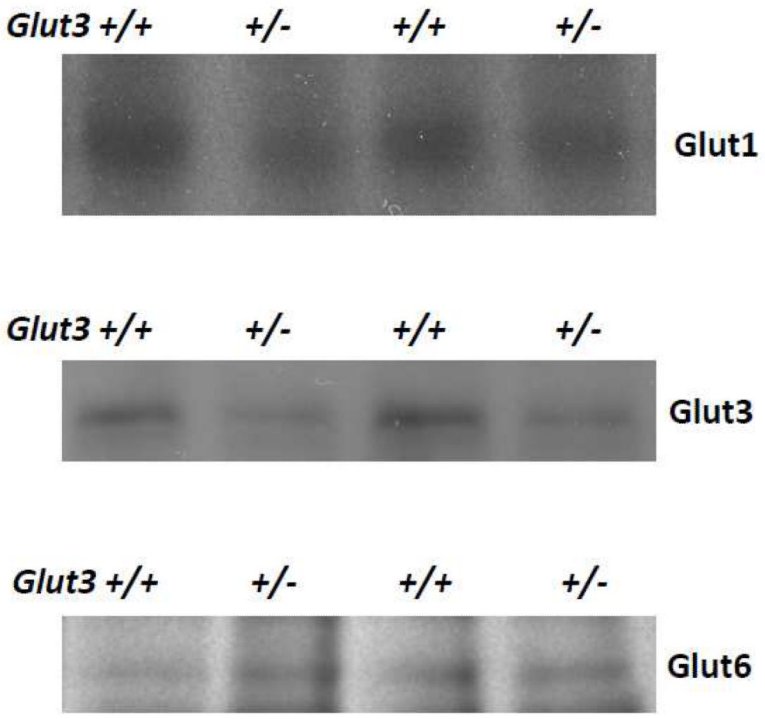

Figure 1. Expression of Glut1, Glut3, and Glut6 in brain homogenate from *Glut3*+/− mice

Shown here are representative immunoblots of brain homogenates subjected to PAGE and probing of resulting membranes with antibodies against mGlut3, hGLUT1, and hGLUT6. Digital image analysis quantified the mean expression of Glut3 at 52% of the Glut3+/+ littermates. The expressions of Glut1 and Glut6 in *Glut3*+/− brain were quantified at 100% and 100%, respectively.

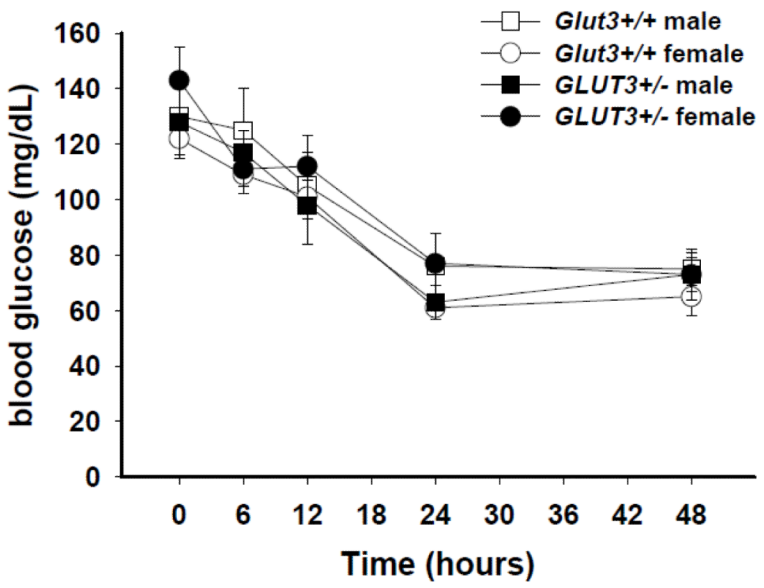

Figure 2. Tolerance to prolonged fasting in mice with *Glut3*+/− genotype

Mice at 10-12 weeks of age were divided into four groups of four animals, male *Glut3*+/−, female *Glut3*+/−, male *Glut3*+/+, and female *Glut3*+/+. After ad lib feeding overnight, food was removed and glucose was determined in blood from a cheek puncture at times 0, 6 hr, 12 hr, 24 hr, and 48 hrs. Each mouse had single blood glucose determinations at five different time separated by one week before the next sequentially increased fasting time period. Ambient temperature was maintained at 29°C to minimize torpor that can occur with food restriction. At no time was there evidence of seizure activity or other change in behavior among the mice during the 48 hours of frequent observation. No significant difference in glucose concentrations was found comparing the groups at any of the durations of fasting.

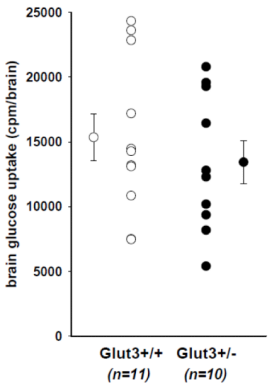

Figure 3. Uptake of glucose into brains of mice with *Glut3*+/− genotype

Ten mice (5 males, 5 females) were injected with 1 μCi of ^{3}H-2-deoxy glucose via tail vein and 45 minutes later were sacrificed by CO_2 inhalation and brain removal. Eleven littermate controls (5 males, 6 females) were similarly evaluated. All animals were allowed free access to food overnight, but food was removed two hours prior to sacrifice. Each brain was removed, rinsed in saline, weighed, and dissolved in Scintigest (Fisher Scientific) at 50°C for at least 18 hours. Brain uptake of glucose was quantified as cpm ^{3}H per brain. Male brains were slightly larger, but there was no difference between the *Glut3*+/− and *Glut3*+/+ groups, whether the data were expressed as cpm/brain or cpm/mg brain.

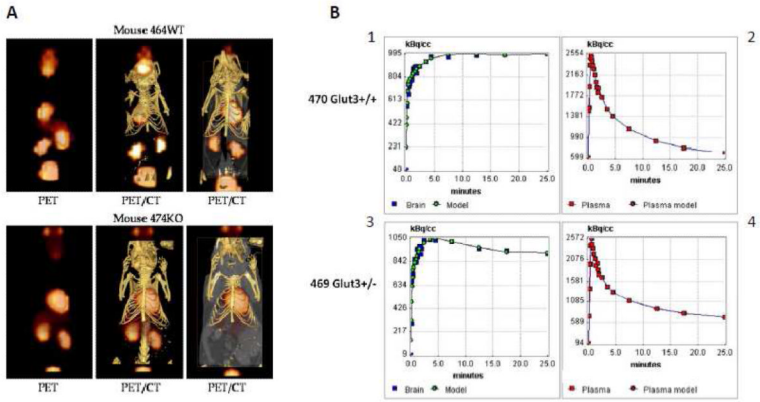

Figure 4. Representative PET/CT images from a *Glut3*+/− and *Glut3*+/+ mouse

Panel A shows examples of PET and PET/CT composite images for a heterozygous mouse (lower images) and a normal littermate. Panel B displays graphs of the time course of brain uptake and blood disappearance of ^{18}F-FDG for a *Glut3*+/+ mouse and a *Glut3*+/− mouse. Graphs 1 and 3 also include points generated using the two-compartment model generated by the kinetic analysis. The kinetic data were indistinguishable between mice with the two *Glut3* genotypes.

Table 1

Summary of kinetic analysis using 1-compartment model

Mouse # (genotype)	X^2	*vB L/L*	*K1 ml/cm^3/min*	*k2 min^{-1}*
462 (Glut3+/−)	7.6	0.464	0.135	0.122
463 (Glut3+/−)	3.2	0.556	0.188	0.072
464 (Glut3+/+)	1.7	0.558	0.233	0.172
468 (Glut3+/+)	9.3	0.531	0.199	0.096
469 (Glut3+/−)	3.4	0.326	0.169	0.166
470 (Glut3+/+)	2.0	0.328	0.167	0.148
474 (Glut3+/−)	2.4	0.284	0.220	0.189
475 (Glut3+/+)	3.6	0.248	0.192	0.176
476 (Glut3+/+)	9.6	0.266	0.340	0.330

Table 2

Summary of kinetic analysis using 2-compartment model

Mouse # (genotype)	*K1* *ml/cm^3/min*	*k2* *min^{-1}*	*k3* *min^{-1}*	*K_{FDG}* *ml/cm^3/min*	*CMR_{gluc}* *μmol/min/100g*
462 (Glut3+/−)	0.590	0.596	0.028	0.0265	29.8 ± 4.1
463 (Glut3+/−)	0.713	0.755	0.049	0.0439	48.3 ± 5.6
464 (Glut3+/+)	0.938	0.861	0.031	0.0326	36.2 ± 7.5
468 (Glut3+/+)	1.099	1.366	0.057	0.0440	48.2 ± 5.0
469 (Glut3+/−)	0.623	0.747	0.042	0.0332	36.6 ± 4.5
470 (Glut3+/+)	0.459	0.531	0.032	0.0261	28.7 ± 3.9
474 (Glut3+/−)	0.569	0.581	0.026	0.0244	26.8 ± 5.4
475 (Glut3+/+)	*0.552*	*0.607*	*0.030*	*0.0260*	*28.7 ± 6.2*
476 (Glut3+/+)	0.607	0.982	0.049	0.0288	32.1 ± 3.2